Supplementary material

Follow-up behavioural experiment

Six additional patients with right-hemisphere lesions, left spatial neglect, and intact visual fields performed two tasks at central fixation, equivalent to the no-load and higher-load conditions in the main fMRI session. These now ran in short alternating blocks (20-40 sec), while object pictures[1] were briefly flashed (250 ms) at unpredictable intervals (every 5-10 sec) in either the left or right hemifield (2-4 pictures on each side during each block type). No response to these objects was required on presentation (analogously to the checkerboards during fMRI). After each pair of blocks (in counterbalanced order, i.e., no-then-high or high-then-no load), recognition was tested by presenting (centrally) the previously shown objects one a time but now intermingled in a sequence with novel items (12 each). Patients had to make an old/new judgment for each of these centrally-presented items. Four to five pairs of blocks were administered to each patient, in different order (after a first pair used for training in the central tasks only, with no surprise recognition test).

The recognition tests revealed that hit-rate was comparable for objects previously exposed in LVF or RVF (35% and 40% respectively) under no-load at fixation; but that higher central load during exposure led to significantly worse recognition for LVF (now 11%) than RVF stimuli (28%). The interaction between central demand and hemifield was reliable across the six patients ($F_{1,5}$=7.5, p=.04). Analogously to the fMRI data, there was thus no difference between visual hemifields under minimal central load (t_5=0.5, n.s), with a visual asymmetry emerging only under increased central load (t_5=3.9, p=0.01).

Eye-tracking during scanning

Continuous eye-tracking was performed during fMRI via infrared camera (ASL 450 LRO system, 60 Hz sampling rate). Data analyzed offline showed correct fixation on the central stimulus stream across all conditions of the attention experiment, as expected given task requirements (mean variance of eye position < 1.15° of visual angle; deviation > 2 degrees away from centre arose only <5.75% of time points, in each patient). Most importantly, eye-position was equivalent across conditions, with a 4 (stimulation) x 2 (task load) ANOVA on mean eye-position coordinates (x or y) showing no significant main effect nor interactions for horizontal (all F<1.33, p>.26) or vertical eye-position (all F<1.67, p>.12). Similarly, for the retinotopic stimulation runs, offline analyses of eye-tracking data showed accurate central fixation and no differences in mean gaze position between the two mapping situations, for both patients.

Reference

1. Snodgrass JG, Vanderwart M: A standardized set of 260 pictures: norms for name agreement, image agreement, familiarity, and visual complexity. *J Exp Psychol [Hum Learn]* 1980, 6:174-215.

Table S1:

Clinical data for each patient in the fMRI study.

	Patient AH	***Patient JC***
Demographic details	Male, 59 year-old, right-handed	Male, 72 year-old, right-handed
Type and time of stroke	Ischemic infarction, 5 months post-onset	Hemorrhage, 2 months post-onset
Neurological deficits	Mild paresis of left arm, no hemianopia, but left neglect	Mild paresis of left hand, no hemianopia, but left neglect
Letter cancellation task	6 omissions / 30 left-sided targets	8 omissions / 30 left-sided targets
Line bisection task	Mean rightward deviation 12 mm for 200mm line	Mean rightward deviation 21 mm for 200mm line

Table S2:
Peaks of load effects within retinotopic ROIs
(for contrast of No Load > Higher Load in initial SPM analysis)

	Right hemisphere		Left hemisphere	
	z-score	*p-value*	*z-score*	*p-value*
Patient AH				
V1	2.53	0.006	0.43	0.334
V2	3.28	0.001	1.16	0.117
V3	3.26	0.001	1.07	0.142
V4	3.61	0.000	-0.15	0.561
Patient JC				
V1	3.49	0.000	-0.30	0.619
V2	3.36	0.000	-0.01	0.506
V3	2.77	0.003	0.46	0.324
V4	3.55	0.000	-0.27	0.607

Legends for supplemental figures

Figure S1.

Anatomy of brain lesions in each patient. Both AH and JC had persistent left spatial neglect after focal right parietal damage (see also Suppl. Table S1). Upper panels: 3D reconstruction of cortical surface (dotted circles indicate the lesions), with oblique view on posterior right hemisphere. Lower panels: horizontal sections (arrows indicate the lesions), with right hemisphere shown on left, following radiological convention. Both lesions also extend subcortically, beyond visible damage to the cortical surface.

Figure S2.

Illustration of retinotopic mapping data for both hemispheres and both patients, projected on flattened views of the occipital cortical surface. These flatmaps are shown here for completeness, since the present study is the first to our knowledge to apply retinotopic mapping in neglect patients. The flatmap data were visualized by combining SPM data with MrGray and MrFlatMesh routines developed by Wandell and colleagues (see Dougherty et al., 2003; Schwarz et al., 2005). Note that our mapping procedure used a standardized short stimulation session (equivalent to that used in normals by Schwartz et al., 2005) that was tolerable for patients, with the aim just to obtain satisfactory demarcation of distinct visual areas, V1, V2, V3 and V4/TEO (but not to measure magnitude or extent of retinotopic activation per se). The rotating wedge and expanding annulus used for retinotopic mapping traversed the same visual angles that could be occupied by checkerboards in the main attention-load experiment (see also Schwartz et al., 2005). Importantly here, mapping results for right visual areas (damaged hemisphere, R) were qualitatively similar to those for left areas (intact side, L). Stimulus-responsive voxels for analysis in the main experiment were selected based on the combination (overlap) of activations to both rotating and expanding stimulations in the visual field (see black outlines of each area in this figure). The mapping data are displayed here with colour codes corresponding to (A) polar angle (i.e. rotation phase of the wedge) or separately (B) eccentricity (i.e. expansion phase of the annulus). Additional analyses (not shown) separated fMRI data for retinotopic ROIs from the main attentional-load experiment in terms of different eccentricity sectors, near or far from central fixation (as in Schwartz et al., 2005). This confirmed that the asymmetrical impact of attentional load (i.e. higher central load reducing visual responses for right visual cortex but not left in neglect patients) applied across all eccentricities here, as per our main analysis that disregards that factor.

Figure S3.

Response of retinotopic areas in right visual areas (beta values, relative to the no-checkerboard baseline, analogous to Fig 2b in main paper) for all conditions with contralateral visual stimulation (unilateral or bilateral checkerboards, now shown separately here), as a function of attentional-load at fixation. In both patients, increased attentional-load reduced the response to contralateral checkerboards in right visual cortex, leading even to elimination of any visual response in right V4/TEO. This was found similarly for unilateral left and bilateral stimulation (i.e., for both conditions that included a left checkerboard projecting to right visual cortex).

Supplemental Data

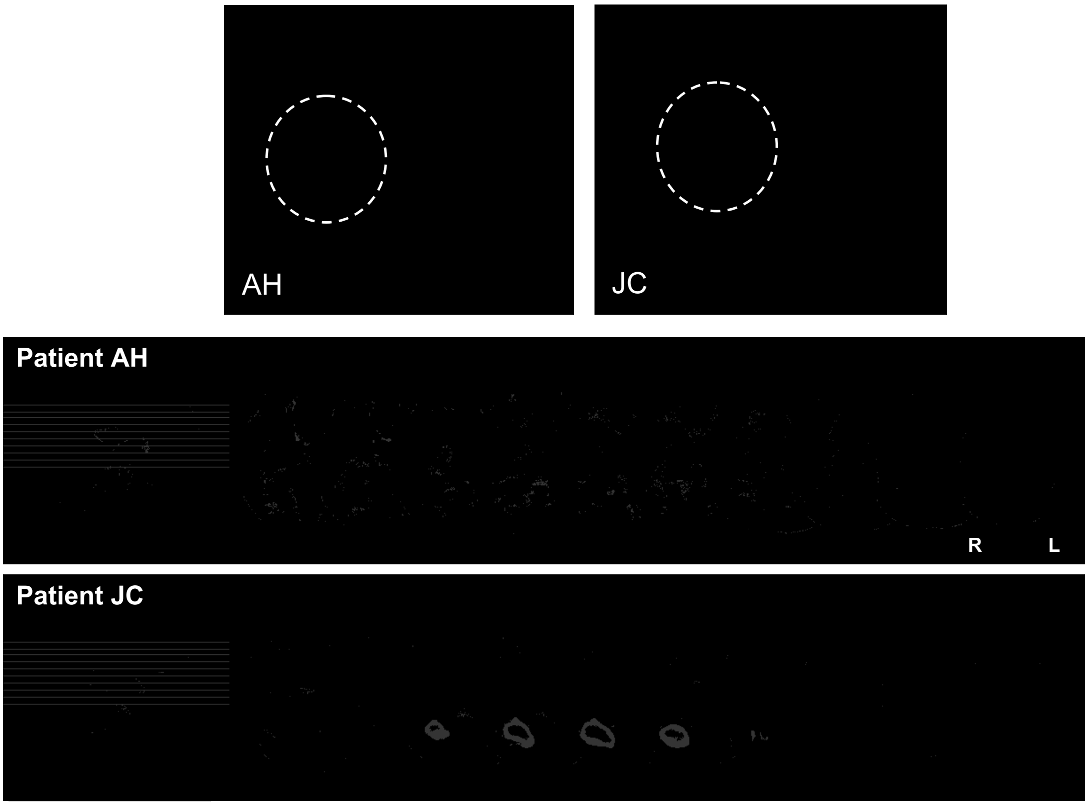

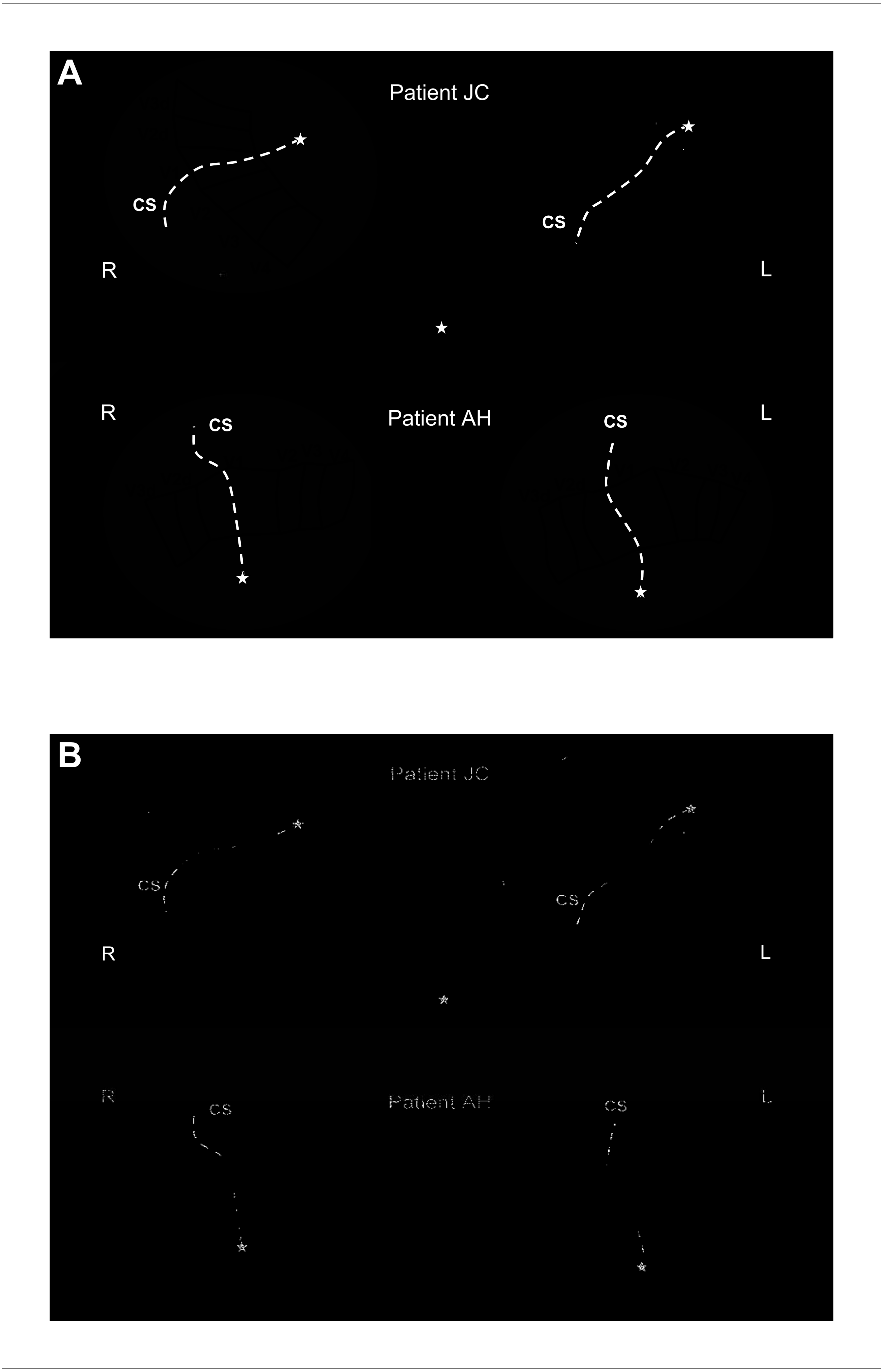
A
Patient JC
CS
CS
R
L
R
Patient AH
L
CS
CS
B
Patient JC
CS
CS
R
L
R
Patient AH
L
CS
CS

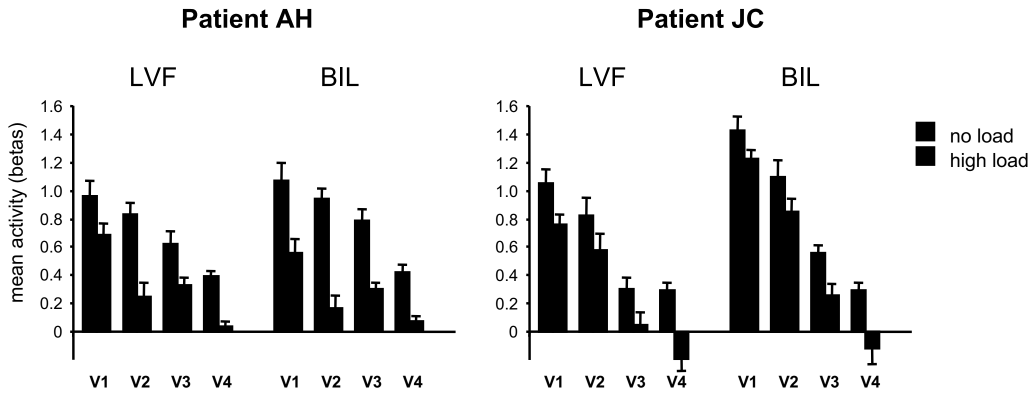
Patient AH
Patient JC
LVF
BIL
LVF
BIL
mean activity (betas)
1.6
1.4
1.2
1.0
0.8
0.6
0.4
0.2
0
V1
V2
V3
V4
no load
high load